


Crotonylation of key metabolic enzymes regulates carbon catabolite repression in *Streptomyces roseosporus*

Chen-Fan Sun^{1,2}, Wei-Feng Xu^{1,2}, Qing-Wei Zhao^{1,3}, Shuai Luo^{1,2}, Xin-Ai Chen^{1,2}, Yong-Quan Li^{1,2}✉ & Xu-Ming Mao^{1,2} ✉

Due to the plethora natural products made by *Streptomyces*, the regulation of its metabolism are of great interest, whereas there is a lack of detailed understanding of the role of post-translational modifications (PTM) beyond traditional transcriptional regulation. Herein with *Streptomyces roseosporus* as a model, we showed that crotonylation is widespread on key enzymes for various metabolic pathways, and sufficient crotonylation in primary metabolism and timely elimination in secondary metabolism are required for proper *Streptomyces* metabolism. Particularly, the glucose kinase Glk, a keyplayer of carbon catabolite repression (CCR) regulating bacterial metabolism, is identified reversibly crotonylated by the decrotonylase CobB and the crotonyl-transferase Kct1 to negatively control its activity. Furthermore, crotonylation positively regulates CCR for *Streptomyces* metabolism through modulation of the ratio of glucose uptake/Glk activity and utilization of carbon sources. Thus, our results revealed a regulatory mechanism that crotonylation globally regulates *Streptomyces* metabolism at least through positive modulation of CCR.

¹Institute of Pharmaceutical Biotechnology & Research Center for Clinical Pharmacy, The First Affiliated Hospital, School of Medicine, Zhejiang University, 310058 Hangzhou, China. ²Zhejiang Provincial Key Laboratory for Microbial Biochemistry and Metabolic Engineering, 310058 Hangzhou, China. ³Zhejiang Provincial Key Laboratory for Drug Evaluation and Clinical Research, 310003 Hangzhou, China. ✉email: lyq@zju.edu.cn; xmmao@zju.edu.cn

S*treptomyces* are profoundly famed as bacterial producers of natural products with diverse chemical structures and bioactivities¹. The short-chain acyl-CoA species, such as acetyl-CoA, malonyl-CoA, and succinyl-CoA, are catabolites from primary metabolism. Meanwhile, they are common precursors and building blocks for biosynthesis of macromolecules in primary metabolism and natural products in secondary metabolism^{2–4}. It has been well recognized that precise control of primary/secondary metabolism development of *Streptomyces* and their switch are critical for the proper production of these invaluable natural products⁵.

Traditionally, regulation of *Streptomyces* metabolism has been extensively studied at the transcriptional levels^{6,7}. But recently, protein acetylation from acetyl-CoA, one of the posttranslational modifications (PTMs), has been shown to be involved in the regulation of production of both primary and secondary metabolites in *Streptomyces*. Acetylation was initially reported in two conserved *Streptomyces* enzymes acetyl-CoA synthetase⁸ and acetoacetyl-CoA synthetase⁹. Following acetyl-proteome assays showed that acetylation is widely distributed in *Streptomyces*, since 667 and 134 proteins were identified acetylated in *S. roseosporus* and *S. griseus*, respectively. Acetylated proteins are mainly involved in metabolism, followed by protein biogenesis and turn-over. Meanwhile, acetylation also occurs on some biosynthetic enzymes for natural products, including the dTDP-4-dehydrorhamnose 3,5-epimerase StrM for streptomycin biosynthesis and the adenylation domain of a non-ribosomal peptide synthase^{10,11}. Interestingly, acetylation of enzymes unexceptionally abolishes their catalytic activities^{8,9,11}. Though regulation of PTMs on the activity of some enzymes has been reported as shown above, how PTMs regulate the *Streptomyces* metabolism in a broader scope has not yet been addressed.

Carbon catabolite repression (CCR) is a conserved mechanism allowing the bacteria, as well as *Streptomyces*, to generally utilize preferred carbon source (such as glucose in laboratory cultivations) over others and attracting the attention as a checkpoint for differentiation of *Streptomyces*¹². Glucose induction often triggers CCR and leads to delayed morphological development and repressed secondary metabolite production^{13–15}. In *Streptomyces*, glucose kinase (Glc) has been shown to be involved in CCR regulation^{16,17}, possibly through its kinase activity to phosphorylate glucose and strengthen glycolysis to produce metabolic intermediates for CCR regulation and through its regulatory activity by interacting with downstream transcriptional regulators^{13,18,19}. It has been proposed that the cytosolic fraction of Glc has a certain kind of PTM for its interaction with regulators, while Glc can also be recruited to the cell membrane to interact with the permease GlcP for glucose metabolism²⁰. Meanwhile, the ratio of glucose uptake/Glc kinase activity has been suggested as a determinant of sensitivity to CCR¹⁸. However, there is no report about which PTM of Glc for CCR regulation on *Streptomyces* metabolism.

To our knowledge, crotonylation is a newly identified PTM on eukaryotic histones²¹. Modification of histones with this unique planar, four-carbon structure, and neutral charge reduces histone–DNA interaction²². Thus histone crotonylation is predominantly found on transcriptionally active regions and enhancers during mouse spermatogenesis²¹, renewal of embryonic stem cells²³, and acute kidney injury²⁴. In addition to its epigenetic modification on histones, crotonylation also occurs in a broad range of non-histone proteins^{25–28} and participates in diverse metabolic pathways such as acetylation²⁹. Crotonylation happens through reversible modifications by enzymes, including crotonyltransferases (writers) and decrotonylases (erasers). Studies have shown that crotonylation has overlapped acyltransferases and de-acylases with acetylation and other types of

acylations^{25,30} and also overlapped modification sites on histones^{29,31}. These findings suggest that crotonylation is a global PTM with a complex interplay with other acylations. Nevertheless, crotonylation in bacteria, as well as how it regulates the bacterial metabolism, has not been reported.

Here we showed that crotonylation is universal in *Streptomyces* metabolic pathways and regulates the metabolism at least through positively modulating CCR, by reversible modifications on Glc. Our work provides comprehensive insights by far, exploring the mechanisms of PTM in regulating *Streptomyces* metabolism, and potentially paves the way for PTM engineering in *Streptomyces* for optimal production of secondary metabolites.

Results

Protein crotonylation is widespread in *Streptomyces*. *Streptomyces* proteins have been found extensively acetylated, and this PTM plays essential roles in enzyme activity modulation for primary/secondary metabolite biosynthesis^{8–11}. Though acetyl-CoA is believed the most abundant acyl-CoA species³², other acyl-CoAs might have more subtle and complex roles in the regulation of *Streptomyces* metabolism.

When exploring the PTM profile of *Streptomyces* proteome throughout the fermentation, we found strong signals from immunoblots with an anti-lysine-crotonyl group (α -Kcr) antibody, as represented by an antibiotic daptomycin producer *S. roseosporus* (Fig. 1a), as well as laboratory model species like *S. coelicolor* M145³³ and *S. lividans* TK24³⁴, and the industrial producers *S. albus* J1074³⁵ and *S. tsukubaensis* L19³⁶ (Supplementary Fig. 1), suggesting that crotonylation occurs widely in *Streptomyces*. In *S. roseosporus*, the signals from cultures at 36 and 48 h were much stronger, when cells were entering secondary metabolism, than that at 24 h or after 48 h, implying that crotonylation increases during primary metabolism development but decreases during secondary metabolism development. The crotonylation dynamics suggested that this PTM might have regulatory roles on *Streptomyces* primary/secondary metabolism development.

Using this antibody, we detected obviously increased crotonylation levels in cells treated with gradient concentrations of sodium crotonate (NaCr). Meanwhile, sodium acetate (NaAc) treatment also resulted in apparently increased crotonylation (Fig. 1b). However, crotonate or acetate treatments had little impact on acetylation or succinylation (Supplementary Fig. 2). These data suggested that crotonylation is more subtle to environmental signals. Furthermore, we examined the dynamics of crotonyl-CoA and acetyl-CoA levels in response to NaCr or NaAc by liquid chromatography–mass spectrometry (LC-MS; Fig. 1c). Increase of crotonyl-CoA concentration was observed only under 20 mM NaCr or NaAc, whereas no obvious increase of the intra-cellular acetyl-CoA was observed, suggesting that acetyl-CoA is resistant to environmental NaAc fluctuation, while intracellular crotonyl-CoA is mainly derived from acetyl-CoA³⁷.

Crotonylation occurs on various metabolic pathways and regulators.

Next crotonyl-proteomics were performed in *S. roseosporus* to identify the substrates for crotonylation. Since proteasome-mediated degradation is one of the major pathways for protein turn-over³⁸, a proteasome-deficient Δ *prcB/A* mutant was constructed (Supplementary Fig. 3) to potentially enrich more proteins with PTMs by immunoprecipitation with the anti-Kcr monoclonal antibody, and crotonylated proteins along with the modified residues were identified by high-performance LC-MS/MS (Fig. 2a). All the distribution of mass error for precursor ions was <0.03 Da, indicating acceptable mass accuracy of the MS

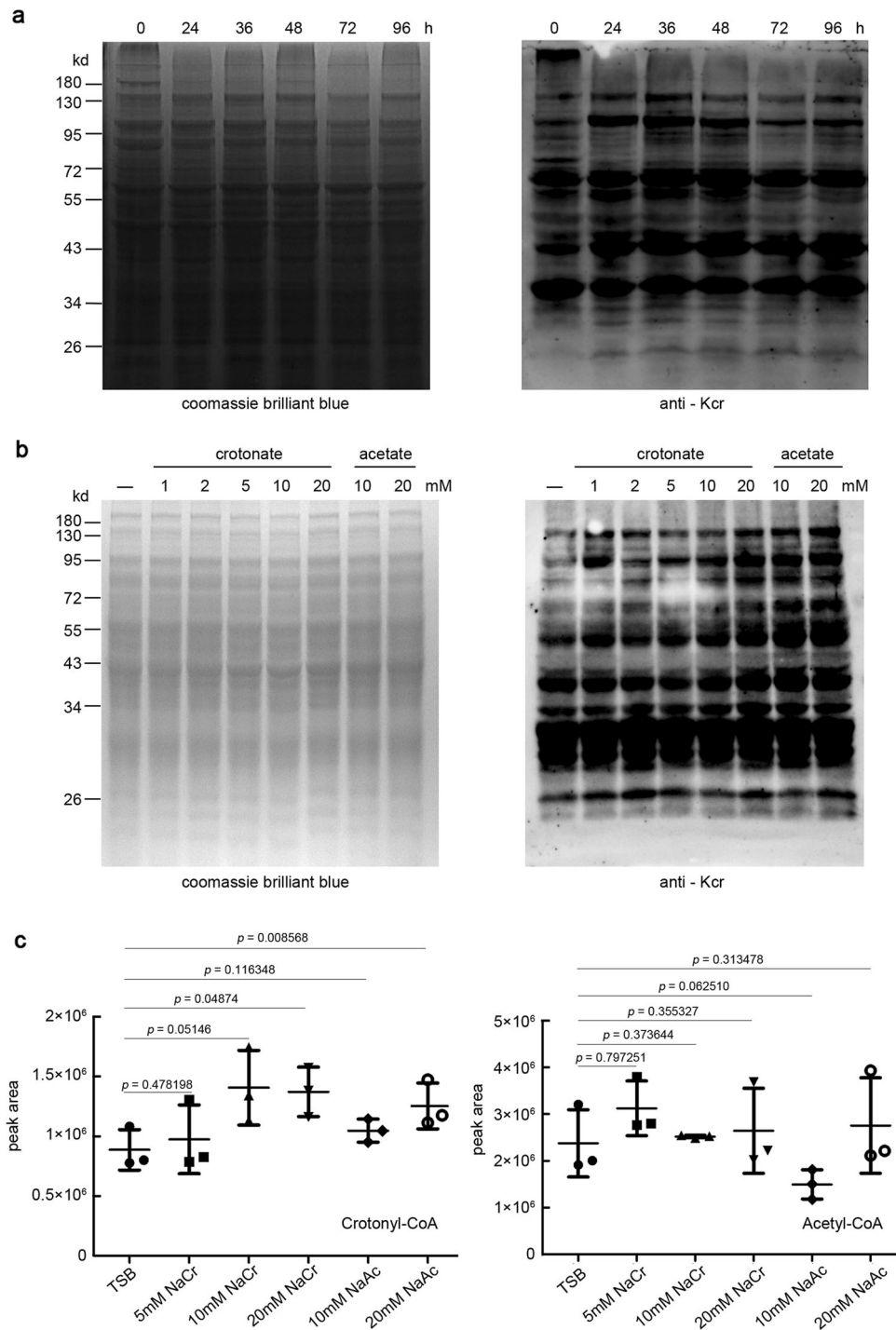


Fig. 1 Crotonylation in *S. roseosporus*. **a** Immunoblot of *S. roseosporus* lysate. Twenty μg of total protein were loaded, and the crotonylated proteins were detected with anti-Kcr monoclonal antibody (1:2000) while Coomassie blue staining was used for the loading control. **b** Immunoblot for crotonylation with anti-Kcr monoclonal antibody (1:2000) in wild-type strain cultured in TSB with additional concentration of sodium crotonate (pH 7.4) or sodium acetate (pH 7.4) as indicated for 24 h. Twenty μg of total protein were loaded, and Coomassie blue staining was used for the loading control. **c** LC-MS analysis of cellular crotonyl-CoA and acetyl-CoA levels from cells cultured as in **b**. The data represent mean peak area \pm SD of three independent experiments. *P* value was calculated with Student's *t* test (ns means $P > 0.05$).

data (Supplementary Fig. 4, Supplementary Data 3). Strikingly, 1389 proteins, along with 3944 lysine residues, were identified with crotonylation, accounting for 19.61% of the putative proteome of *S. roseosporus* (Fig. 2b) (Supplementary Data 2 and 3). It was a contrast to the previous acetyl-proteomic survey in the same species *S. roseosporus* NRRL 11379, where 667 acetylated proteins and 1143 modification sites were identified¹⁰.

Gene ontology (GO) analysis (Supplementary Fig. 5, Supplementary Data 4) showed that 672 crotonylated proteins (34%) are involved in the metabolic processes (Fig. 2c), while 691 crotonylated proteins (50%) are enzymes with catalytic activities (Fig. 2d), suggesting that crotonylation primarily regulates enzymatic activities in *S. roseosporus* metabolism. Consistent with these observations, Kyoto Encyclopedia of Genes and

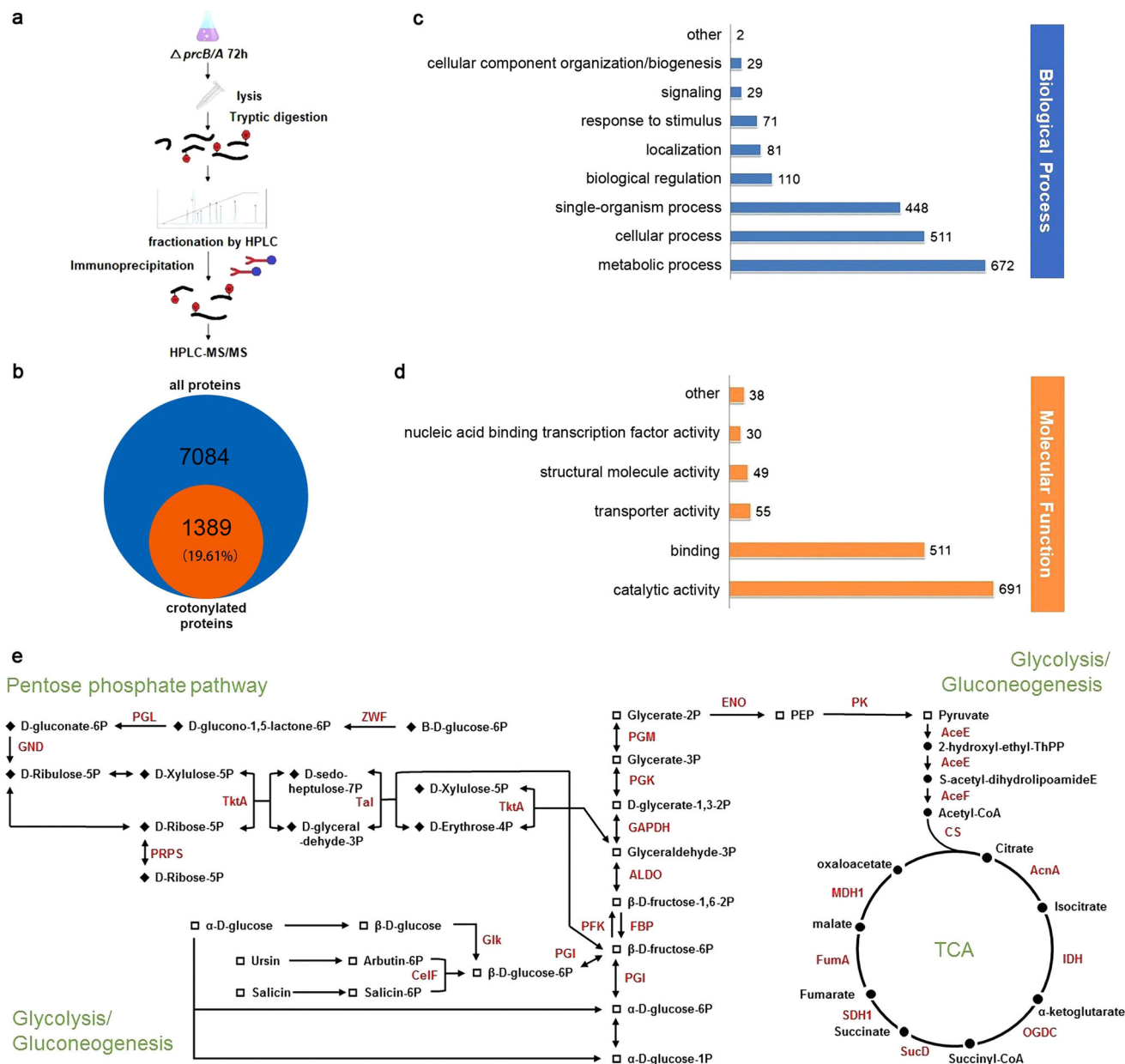


Fig. 2 Crotonyl-proteomic analysis of *S. roseosporus* proteins. **a** Procedure diagram for crotonyl-proteomics in *S. roseosporus*. **b** Statistics of crotonylated proteins from *S. roseosporus*. **c, d** Gene ontology functional classification of the identified crotonylation proteins based on biological processes (**c**) and molecular functions (**d**). **e** Carbon metabolism pathways in *Streptomyces*. Crotonylated enzymes are highlighted in red.

Genomes (KEGG) analysis (Supplementary Data 5) showed that most enzymes in carbon metabolism are crotonylated (Supplementary Fig. 6). Particularly, all enzymes in glucose catabolism, including glycolysis, pyruvate dehydrogenation, and tricarboxylic acid cycle (TCA) (Fig. 2e, Supplementary Figs. 7 and 8), and most enzymes in oxidative phosphorylation are highly crotonylated (Supplementary Data 5). These data strongly suggested that crotonylation globally regulates glucose utilization, respiratory chain, and potentially production of primary metabolites, such as acetyl-CoA, NADH, NADPH, and ATP. Other critical metabolic pathways in primary metabolism strongly regulated by crotonylation are DNA replication and repair, RNA biogenesis and degradation, protein biogenesis, and turn-over. It has been found that DNA polymerase, topoisomerase, gyrases and UvrABC, RNA polymerase and ribonucleases, most ribosomal proteins, almost all aminoacyl-tRNA synthetases, three chaperones, and protein

degradation system (protease Clp, Lon, proteasome components) are heavily modified (Supplementary Figs. 9 and 10, Supplementary Data 3). Moreover, some acyl-CoA synthetases, including acetyl-CoA synthetase AcsA, are also crotonylated, but interestingly, no de-acylases are found modified with crotonylation (Supplementary Data 3), suggesting that crotonylation might modulate the biogenesis and intracellular concentrations of acyl-CoAs.

Meanwhile, regulators for secondary metabolism development were also found crotonylated, such as the putative γ -butyrolactone receptor ArpA^{39,40}, the intracellular ppGpp synthase RelA⁴¹, and the nutrient-responsive regulators GlnR⁴², PhoP⁴³, and AtrA⁴⁰ (Supplementary Data 3). More interestingly, crotonylation was also found on some biosynthetic enzymes for natural products, such as DptE, DptA, and DptD, the core enzymes in biosynthesis of daptomycin (Supplementary Data 3),

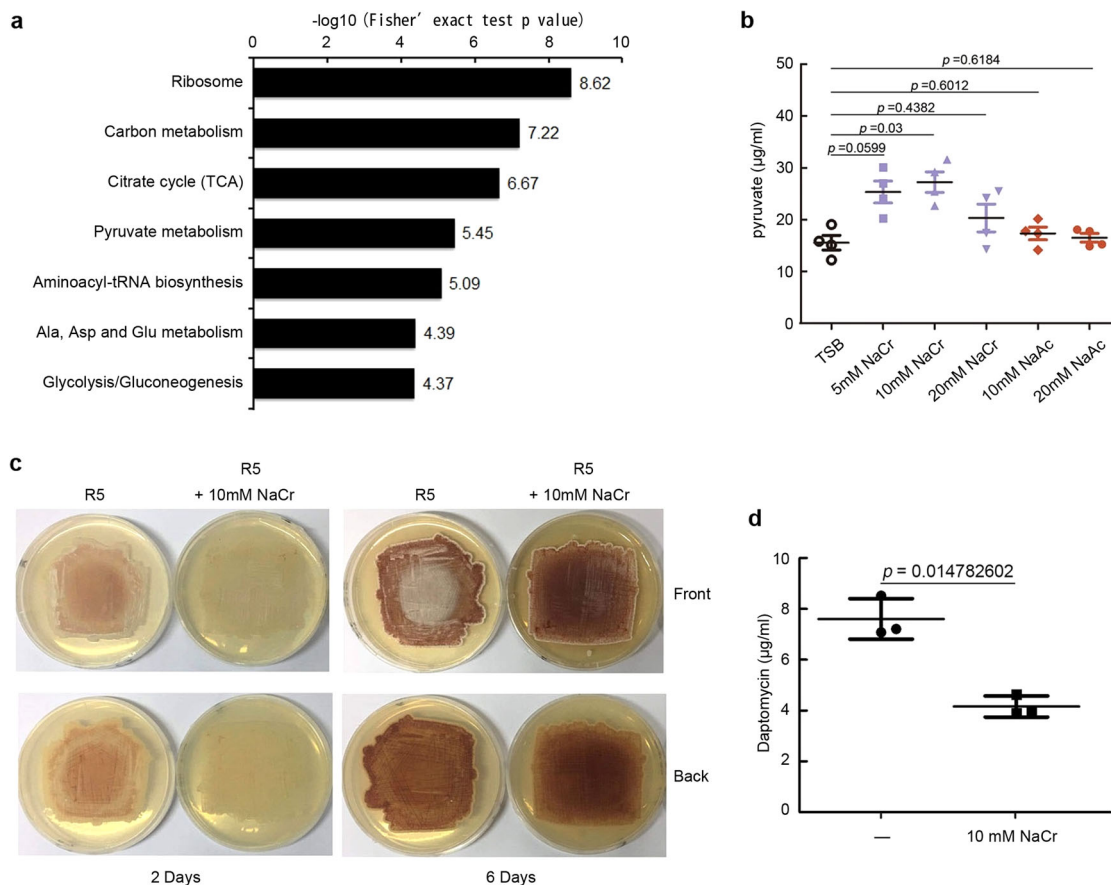


Fig. 3 Crotonylation regulates *S. roseosporus* metabolism. **a** KEGG pathway-enrichment analysis for lysine-crotonylated proteins. **b** Pyruvate production assays with addition of NaCr or NaAc. *S. roseosporus* wild type was cultured in TSB supplemented with NaCr (pH 7.4) or NaAc (pH 7.4) with the indicated concentrations for 24 h, and the intracellular pyruvate concentration was determined. *P* value was calculated with Student's *t* test ($n = 4$). **c** Morphological phenotype of *S. roseosporus* wild type on R5 with or without 10 mM NaCr (pH 7.4) for 2 or 6 days. **d** Daptomycin production in wild type supplemented with 10 mM NaCr. The daptomycin yield was measured after culturing 120 h. Experiments were performed in triplicate. *P* value was calculated with Student's *t* test ($n = 3$).

a representative antibiotic produced by *S. roseosporus*^{40,44}. All these data suggested that crotonylation globally occurs on key metabolic enzymes, biosynthetic enzymes, and critical regulators and thus might regulate metabolism of *Streptomyces*.

Among all PTMs identified to date, acetylation has been extensively mapped in diverse organisms. We compared the crotonylation substrates identified in our study to previously determined acetyl-proteome in *S. roseosporus*¹⁰. We found that 37% of crotonylated proteins are acetylated as well at their Lys residues (Supplementary Fig. 11a). Meanwhile, these two acylations possess priority of various modification-occurring motifs (Supplementary Fig. 11b). Further KEGG pathway enrichment (Supplementary Fig. 11c) and protein domain enrichment (Supplementary Fig. 11d) of these two modifications suggested that the most enriched categories for crotonylated proteins were ribosome ($p = 2.40E-09$) and carbon metabolism, such as citrate cycle ($p = 2.14E-07$), glycolysis/gluconeogenesis ($p = 4.22E-05$), and pyruvate metabolism ($p = 3.59E-06$) (Supplementary Fig. 11c), whereas they were aminoacyl-tRNA biosynthesis ($p = 2.33E-06$) and ribosome ($p = 3.19E-05$) for acetylation.

Crotonylation regulates *Streptomyces* metabolism. Next, we further investigated the regulatory roles of crotonylation for *Streptomyces* metabolism. In the KEGG metabolic pathway analysis (Fig. 3a), the top enriched categories for lysine-crotonylated

substrates were ribosome and carbon metabolism, such as TCA cycle, while the top categories of acetylation were aminoacyl-tRNA biosynthesis, ribosome in our strain as well as *S. erythraea*⁴⁵, and ribosome and pyruvate metabolism for succinylation in *Escherichia coli*⁴⁶, implying a possible link between crotonylation and carbon metabolism. Consistently, increased production of pyruvate was observed at the supplement of 10 mM NaCr, but not at 5 or 20 mM NaCr or with addition of NaAc (Fig. 3b). Considering an incremental level of crotonylation during primary metabolism (Fig. 1a), these results suggested that proper enhancement of crotonylation might benefit *Streptomyces* during primary metabolism, but excessive modification would be backfired. Meanwhile, we observed delayed aerial mycelium development (Fig. 3c) and postponed secondary metabolism development for red pigment production (Fig. 3c) and daptomycin production (Fig. 3d) if cells were supplemented with 10 mM NaCr. These observations experimentally suggested that crotonylation is involved in the regulation of both primary and secondary metabolism of *Streptomyces*.

Identification of modification enzymes for *Streptomyces* crotonylation. Next, we tried to identify enzymes responsible for this PTM. Protein crotonylation is reversibly catalyzed by crotonyl-transferase (writers) and decrotonylase (erasers)^{25,47}, and the canonical acetyltransferase p300 in mammalian cells also acts as a crotonyl-transferase^{21,32,48}, suggesting that some enzymes are

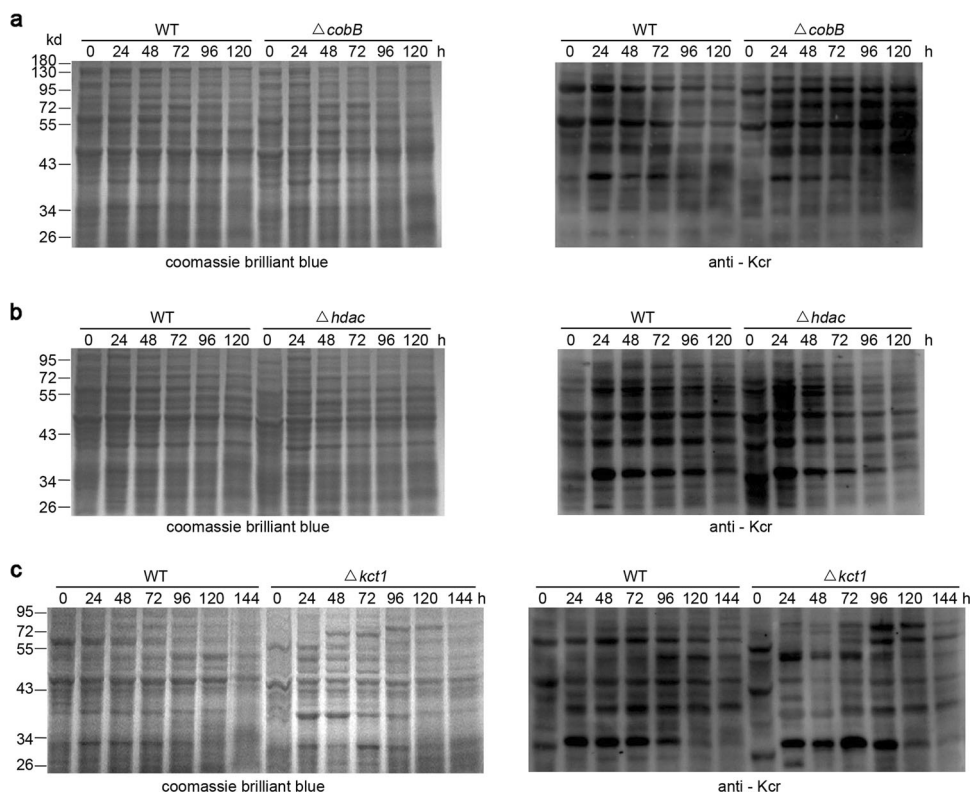


Fig. 4 Identification of crotonylation enzymes. Immuno-blot assays of crotonylation with anti-Kcr monoclonal antibody (1:2000) from *S. roseosporus* strain wild type (WT), two decrotonylase mutants $\Delta cobB$ (a) and $\Delta hdac$ (b), and a crotonyl-transferase mutant $\Delta kct1$ (c) with anti-Kcr monoclonal antibody in right, together with Coomassie blue staining in left for the loading control.

pluripotent in acyl-modifications. In *Streptomyces*, two deacetyl-transferases, the NAD^+ -dependent deacetylase CobB and Zn^{2+} -dependent deacetylase histone deacetylase (HDAC), and a putative GCN5-family acetyl-transferase Kct1, have been well characterized⁴⁹ and are highly conserved (Supplementary Figs. 12–14). We found that removal of these homologs in *S. roseosporus* showed remarkable alterations of crotonylation (Supplementary Figs. 15–17). The $\Delta cobB$ mutant displayed constitutively higher crotonylation during fermentation, particularly after 48 h, than the wild type, whose modification obviously dropped at that time (Fig. 4a and Supplementary Fig. 18a). The $\Delta hdac$ mutant showed more crotonylation in the early developmental phases but lower modification after 48 h compared to the wild type (Fig. 4b and Supplementary Fig. 18b). These data genetically confirmed that both CobB and HDAC work as decrotonylases in *S. roseosporus*, but they primarily function in different developmental stages. HDAC is responsible for the maintenance of low crotonylation in the primary metabolism, while CobB mainly works in the later phases of secondary metabolism. Moreover, deletion of *kct1* caused decreased crotonylation as expected, especially in the early stages before 72 h (Fig. 4c and Supplementary Fig. 18c), but similar protein modification was observed after 72 h between wild type and the $\Delta kct1$ mutant, genetically confirming that Kct1 is a crotonyl-transferase.

Consistent with the altered crotonylation profiles, both $\Delta cobB$ and $\Delta hdac$ mutants showed more biomass than wild type, while $\Delta kct1$ mutant had retarded growth before 72 h but restored afterwards Supplementary Fig. 19a), further suggesting that sufficient crotonylation in the early phases benefits cell vegetative growth, which was in agreement with the gradually increased crotonylation observed in wild type. Consistently, over-produced pyruvate and ATP in both $\Delta cobB$ and $\Delta hdac$ mutants but a decreased ATP concentration in the $\Delta kct1$ mutant was observed

(Supplementary Fig. 19b). But interestingly, statistically increased production of crotonyl-CoA and decreased production of acetyl-CoA were observed in $\Delta hdac$ and $\Delta cobB$ mutants, respectively (Supplementary Fig. 19c). Furthermore, both decrotonylase mutants began to produce the secondary metabolite daptomycin at 48 h, earlier than wild type. But it was noteworthy that, though similar daptomycin titers were observed in $\Delta cobB$ mutant and wild type at 72 and 96 h, the metabolite production in $\Delta cobB$ mutant dropped much faster afterward, while the $\Delta hdac$ mutant showed constitutively higher productivity (Supplementary Fig. 19d), implying that excessive crotonylation in the early phases might benefit production of secondary metabolites, but crotonylation should be partially erased for proper metabolic development in the later phases. This hypothesis could also explain the observation in wild type, where crotonylation gradually increased before 36 h but slowly dropped after 48 h. Consistently, the $\Delta kct1$ mutant with weakened crotonylation only initiated daptomycin production at 96 h and constantly showed a much lower yield of daptomycin throughout the fermentation (Supplementary Fig. 18d). These data supported that delayed crotonylation postpones cell development and reduces secondary metabolite production.

Some writers and erasers in bacteria are versatile in modifications of proteins with various acylations. For examples, CobB has been shown as a de-acetylase in *E. coli* and as a dehydroxybutyrylase in *Proteus mirabilis*⁵⁰. Acetylation and succinylation are two representative PTMs in bacteria. However, we found that, in *S. roseosporus*, $\Delta cobB$ mutant had no obvious change in acetylation profile but showed much higher succinylation, while $\Delta hdac$ mutant had stronger signals both in acetylation and succinylation (Supplementary Fig. 20a). Moreover, no distinct changes were observed in $\Delta kct1$ mutant (Supplementary Fig. 20b). All these data suggested that both erasers also function

in other types of acylation of *Streptomyces*, while the writer Kct1 not (Supplementary Fig. 20c). Though we could not exclude the possible involvement of acetylation or succinylation for metabolic changes of $\Delta cobB$ and $\Delta hdac$ mutants, our observations from $\Delta kct1$ mutant and phenotypes with NaCr addition still supported regulation of crotonylation on *Streptomyces* metabolism.

Glk is reversibly crotonylated by CobB and Kct1. To better understand the molecular regulatory mechanism of crotonylation and further confirm that above phenotypic alterations on *Streptomyces* metabolism authentically result from crotonylation, we looked for critical substrates that are crotonylated but not acetylated and mediate the regulation of crotonylation on *Streptomyces* metabolism. Here we focused on Glk, due to the global modification of glucose catabolism pathway (Fig. 2e) and given that Glk is the first enzyme to activate glucose and a key regulator of CCR in *Streptomyces*^{16,20}. Moreover, Glk was identified crotonylated at two conserved residues K89 and K91 based on MS/MS data (Fig. 5), adjacent to a catalytic D105⁵¹. But interestingly, no acetylation was found on Glk, which thus excludes the influence of acetylation on Glk in our study.

To identify the enzymes that modify Glk, we constructed a bacterial two-hybrid library comprising 54 putative acyl-transferases and 2 de-acylases as the preys (Supplementary Data 6), while Glk was the bait in this system. Interestingly, CobB and Kct1 were screened out from this library to specifically interact with Glk, since the blue lawn was observed only when Glk co-existed with CobB or Kct1 in one bacterial cell to activate the expression of β -galactosidase in the bacterial two-hybrid system (Fig. 6a). Glk, CobB, and Kct1 were expressed and purified from *E. coli*. Based on the immunoblots with α -Kcr antibody, we found that the purified Glk protein has already been modified with crotonylation (Fig. 6b and Supplementary Fig. 21a, Fig. 6c and Supplementary Fig. 21b). In our in vitro assays, Glk can be further crotonylated with crotonyl-CoA in an enzyme-independent pathway for PTM. However, strong crotonylation was observed only when the acyl-transferase Kct1 was further added, confirming that Glk can be crotonylated by Kct1 (Fig. 6b and Supplementary Fig. 21a). Moreover, when Glk was incubated with CobB and the co-factor NAD⁺, decreased crotonylation was observed with about 27% loss for 1 h and over half for 1.5 h (Fig. 6c and Supplementary Fig. 21b), confirming that CobB is an NAD⁺-dependent decrotonylase to erase crotonylation on Glk.

Glk activity is regulated by crotonylation. Next, the effects of crotonylation on Glk kinase activity were evaluated. As shown from in vitro assays in Fig. 7a, we found that Glk with higher crotonylation (modified by Kct1 as in Fig. 6b) had lower activity than the native one purified from *E. coli*, which could recover after decrotonylation by CobB (Supplementary Fig. 22a), suggesting that crotonylation reduces Glk activity. Consistent with this observation, crotonylation mimic of these sites by K to Q single mutation also reduced the activity, and the double mutant had a much lower level of kinase activity (Fig. 7a). Consistent with these observations, when Δglk mutant was complemented with wild-type Glk protein, the constitutively modified Glk (K8991Q) and the unmodified form (K8998R), we found that K–Q mutation led to lower levels of Glk activity, while K–R mutation accounted for the higher kinase activity based on the whole-cell lysate assays (Supplementary Fig. 22b, c).

Further in vivo investigation of crotonylation in wild type showed that crotonylation of Glk increased during cell metabolism development. In primary metabolism (12 and 18 h), the modification was low but sharply increased at 24 h and moderately increased at 48 and 72 h. However, the lowest

crotonylation was observed at 18 h (Fig. 7b and Supplementary Fig. 23a and Fig. 7c and Supplementary Fig. 23b). The dynamics of Glk modification in wild type also correlated to the kinase activity during cell development. Higher activity was observed at primary metabolism, and cells at 18 h had the highest Glk kinase activity (Fig. 7d). These phenomena were well coincident with the previous report in *S. coelicolor* that Glk activity had a peak at 18 h but dropped and was constant afterward²⁰. Interestingly, constitutive hyper-crotonylation of Glk was found in the $\Delta cobB$ mutant throughout the cell development. Especially at 12 and 18 h, this mutant had even much higher modification than wild type from the late development phases (Fig. 7b). This excessive modification of Glk in the $\Delta cobB$ mutant accounted for the lower activity (Fig. 7d). Moreover, ultra-low modification of Glk was found in the $\Delta kct1$ mutant in all developmental phases, and it was almost undetectable at 18 h (Fig. 7c). As expected, we observed much higher Glk activity in this mutant, particularly at 18 h (Fig. 7d). All these data suggested that crotonylation negatively regulates Glk kinase activity, and the in vivo precise proportion between crotonylation and Glk activity dynamics also suggested that crotonylation might be one of the major PTM mechanisms for Glk activity regulation.

Positive modulation of CCR by crotonylation. CCR is a conserved regulatory mechanism to utilize one carbon source (such as glucose) to suppress the metabolism of other carbon sources and *Streptomyces* metabolism, and mainly depends on Glk^{5,13,14}. Glk kinase activity is required for glucose activation and subsequent glycolysis. It has been shown that there was a global loss of CCR in the *glk*-deletion strain⁴, but both Glk-dependent and independent pathways have been proposed for CCR^{16–19}. However, one possible mechanism of Glk on CCR has been proposed that Glk might interact with other transcriptional factors after it is posttranslationally modified²⁰. So we further investigated whether crotonylation influences CCR in *Streptomyces*.

Glucose has been shown to trigger CCR in *Streptomyces* for sugar metabolism, cell differentiation, and secondary metabolite production⁵². First, the residual glucose in the culture was examined. We found that glucose was consumed faster in the $\Delta cobB$ mutant (Fig. 8a), though the Glk activity was much lower (Fig. 7d), while the $\Delta kct1$ mutant showed more glucose surplus than wild type (Fig. 8a). These data indicated that the ratio of glucose uptake/Glk kinase activity was highest in the $\Delta cobB$ mutant but lowest in the $\Delta kct1$ mutant, suggesting that the $\Delta cobB$ mutant had the strongest CCR, while the $\Delta kct1$ mutant had the weakest CCR, according to the index of glucose uptake/Glk activity ratio suggested previously¹⁸. In addition, considering that over-crotonylation of bacterial proteins is the direct consequence in the $\Delta cobB$ mutant, our data suggested that crotonylation should positively regulate CCR.

To further confirm this hypothesis, we investigated the utilization of non-fermentable carbon sources (herein galactose) in the $\Delta cobB$, $\Delta kct1$, and Δglk mutants complemented with Glk or its point mutants to mimic the crotonylated form (K8991Q) or non-crotonylated form (K8991R). The transcription levels of *galK*, a gene encoding galactokinase⁵³ for galactose utilization, were examined. We found repressed *galK* expression in the presence of glucose (Fig. 8b), but it was strongly de-repressed in $\Delta kct1$ mutant (Fig. 8c) or with the non-crotonylated form of Glk (K8991R), even in the presence of glucose (Fig. 8d), suggesting loss of CCR controls. However, *galK* expression was further repressed in the $\Delta cobB$ mutant (Fig. 8c) or when Glk (K8991Q) mutant protein was complemented even in the absence of glucose (Fig. 8d), suggesting the strengthened CCR effects. These results suggested that crotonylation on K89/K91 of Glk is required for

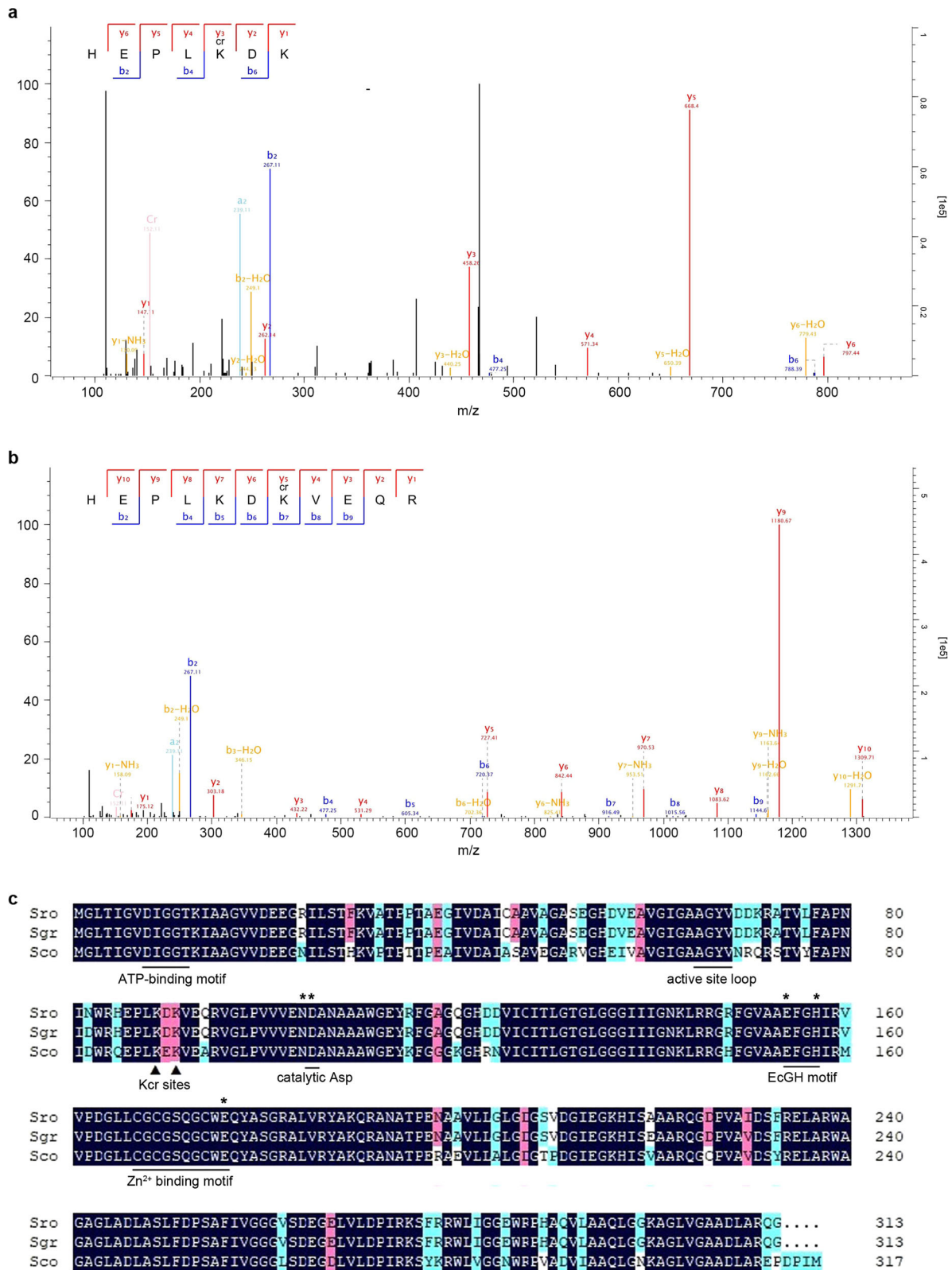


Fig. 5 Glk is crotonylated at two conserved lysine (K) residues. **a** MS/MS analysis of crotonylation on Glk K89. Crotonylation was calculated based on the molecular weight difference values between y3 and y2 (458.26 – 262.14 = 196.12), and b6 and b4 (788.39 – 477.25 = 311.14). **b** MS/MS analysis of crotonylation on Glk K91, which was calculated based on the molecular weight difference values between y5 and y4 (727.41 – 531.29 = 196.12), and b7 and b6 (916.49 – 720.37 = 196.12). **c** Glk protein alignment from *S. roseosporus* (Sro), *S. griseus* (Sgr), and *S. coelicolor* (Sco). Two crotonylated residues (Kcr sites) along with conserved motifs are shown. Residues involved in the glucose-binding mechanism were labeled with asterisks.

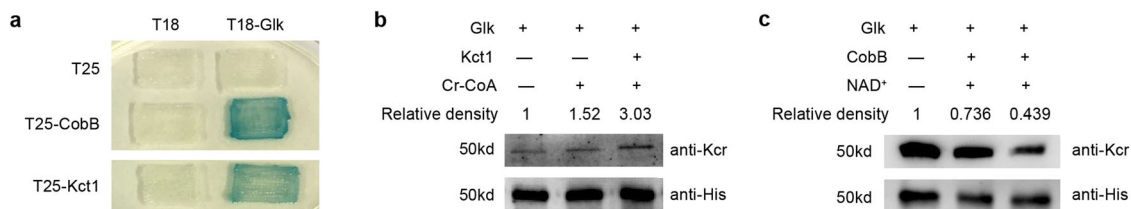


Fig. 6 Glk is reversibly crotonylated by CobB and Kct1. **a** Bacterial two-hybrid analysis of the interaction between Glk and CobB or Kct1. Glk was constructed in pT18, while CobB or Kct1 in pT25. *E. coli* strain BTH101 containing the hybrids were cultured on LB for 48 h and photographed. **b, c** In vitro assays for Glk crotonylation by Kct1 (**b**) and decrotonylation by CobB (**c**). Reactions were analyzed by western blot with the indicated antibodies (1:2000). The relative intensity of each sample is also shown. In **b**, the reaction time is 1 h, while in **c**, the reaction time for decrotonylation is: lane 1, 1.5 h; lane 2, 1 h; lane 3, 1.5 h.

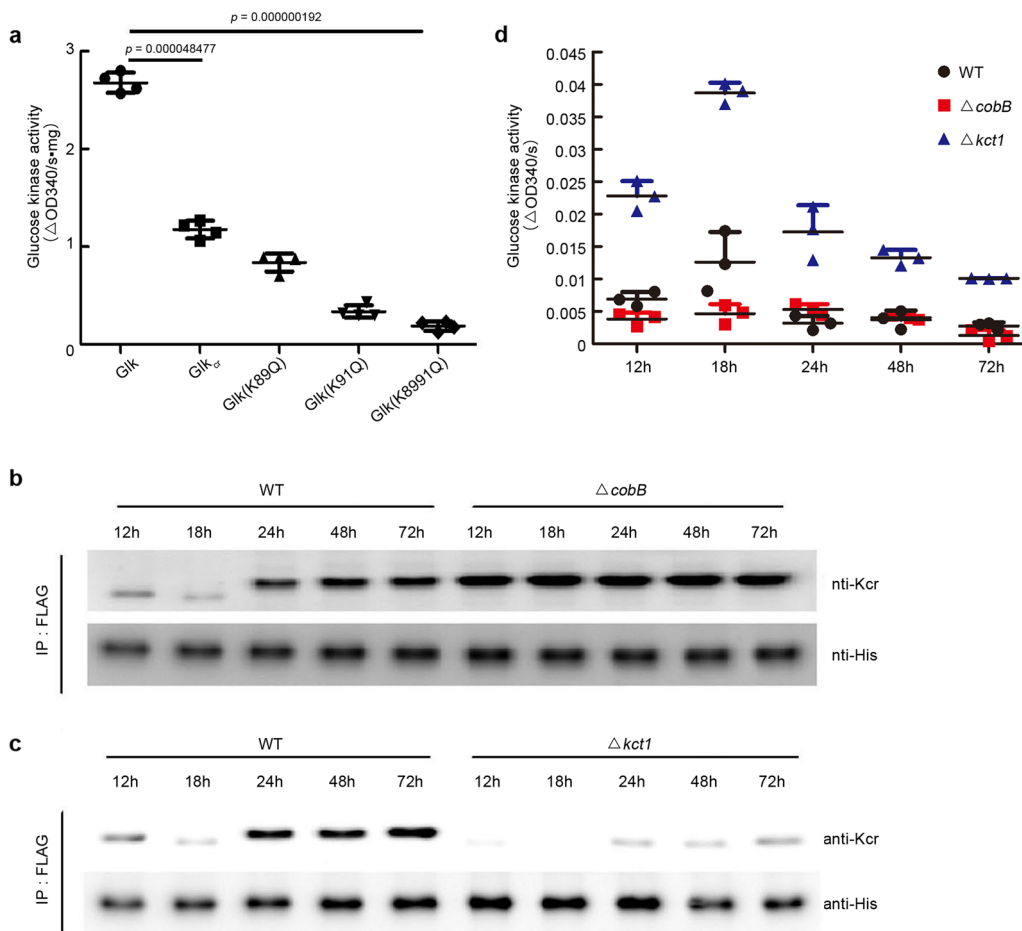


Fig. 7 Crotonylation regulates Glk activity. **a** In vitro assays of crotonylation on the Glk catalytic activity. Glk_{cr} was prepared from the in vitro reaction with Glk and Kct1 in Fig. 3b. Glk mutant isoforms were purified from the in vitro reaction with Glk and Kct1 in Fig. 3b. Glk mutant isoforms were purified from *E. coli*. Statistical significance was determined by two-tailed unpaired Student's *t* test ($n = 4$). **b, c** Western blot analysis of crotonylation level of Glk in vivo. *S. roseosporus* wild type and $\Delta cobB$ and $\Delta kct1$ mutants expressing *ermEp⁺-3flag-glk* were cultured in the YEME medium, and mycelia were taken at the time points indicated. 3FLAG-Glk was immune-precipitated from the lysate, and western blots were performed with anti-FLAG M2 or anti-Kcr rabbit antibody (1:2000). **d** Glucose kinase activity assays of the lysate from wild type and $\Delta cobB$ and $\Delta kct1$ mutants. Bacterial strains were cultured in the YEME medium, and the kinase activity was measured every 12 h. Experiments were performed in triplicate.

proper CCR, and removal of this PTM could constitutively release cells from CCR. Consistent with this hypothesis, the growth defect of $\Delta kct1$ mutant, in which crotonylation of Glk apparently reduced, was rescued to a comparable level of wild type if galactose was the sole carbon source (Fig. 8e). All these data suggested that crotonylation positively regulates CCR in *Streptomyces*.

Discussion

Crotonylation of *Streptomyces* metabolic pathways and enzymes.

Here, based on crotonyl-proteomics, we showed several characteristics of protein crotonylation in *Streptomyces*. First, *Streptomyces* proteins are highly posttranslationally modified as crotonylation. About 20% proteins and 4000 lysine sites in *S. roseosporus* are crotonylated, which is about 2-fold in protein and

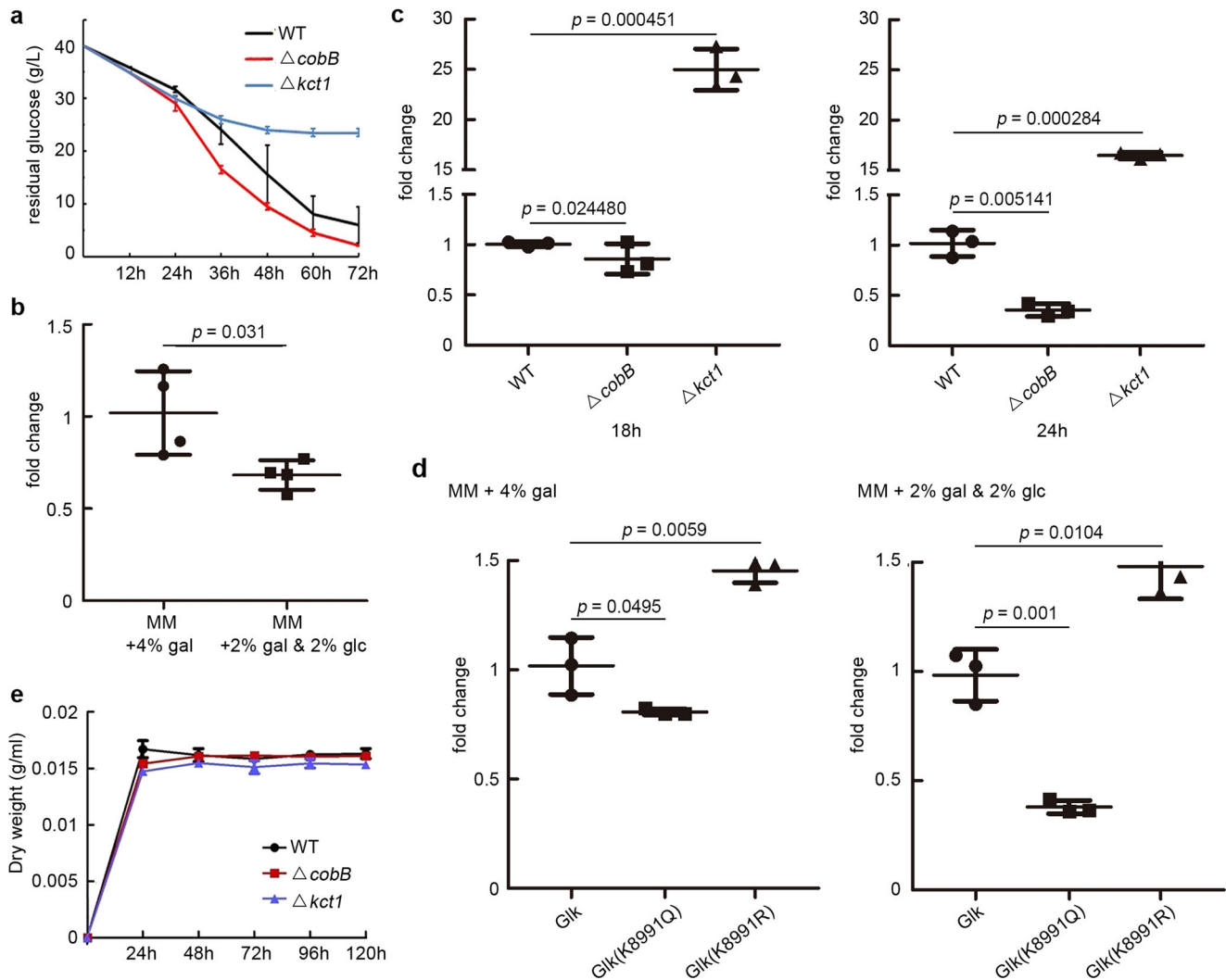


Fig. 8 Crotonylation regulates carbon utilization in *S. roseosporus*. **a** Residual glucose in the medium of *S. roseosporus* wild type and $\Delta cobB$ and $\Delta kct1$ mutants. Bacterial strains were cultured in the YEME medium, and glucose concentration was measured every 12 h. Experiments were performed in triplicate. **b** Quantitative assays of fold change of *galK* gene expression in Δglk mutant complemented with *glk*. Cells were cultured in MM media with different carbon sources. Gal galactose, glc glucose. Experiments were performed in quadruple. **c** Quantitative assays of fold change of *galK* gene expression in wild type and $\Delta cobB$ and $\Delta kct1$ mutants. Cells were cultured in YEME medium with 4% glucose for 18 or 24 h. Experiments were performed in triplicate. **d** Quantitative assays of fold change of *galK* gene expression in Δglk mutant complemented with *glk* and its mutants (K8991Q, K8991R). Cells were cultured in MM media with different carbon sources for 24 h. Gal galactose, glc glucose. Experiments were performed in triplicate. **e** Dry weight of wild type and $\Delta cobB$ and $\Delta kct1$ mutants in the YEME culture without glucose but with galactose as the sole carbon source.

over 3-fold in the site of acetylation in the same species¹⁰. Considering that acetyl-CoA is the most abundant acyl-CoA within cells and estimated 1000-fold more than crotonyl-CoA³², our results suggested that crotonylation might play more broad and sensitive roles than acetylation in *Streptomyces*. Second, though crotonylated proteins are distributed in various cellular processes, such as cell cycle, growth, division, and cellular response to stimulus, most crotonylated proteins are enzymes with catalytic activities and involved in metabolic pathways, mainly in carbon metabolism and protein turn-over. For example, heavily crotonylated enzymes are enriched in glycolysis, pyruvate metabolism, TCA, phospho-pentose pathway, and CoA biogenesis, which are responsible for glucose catabolism, acetyl-CoA, and NAD(P)H production. These observations implied that crotonylation might regulate carbon utilization and biogenesis of acyl-CoA species, thus causing complex interplay of crotonylation with other acyl-CoAs both at intracellular concentrations and their possible competitive modifications. Moreover, almost all aminoacyl-tRNA synthetases,

numerous ribosomal proteins and protein degradation machineries (proteases, proteasome) are also highly crotonylated, suggesting that crotonylation is one of the determinants for protein turn-over in cell metabolism regulation. Third but not the last, crotonylation is involved in secondary metabolism, including cell differentiation and secondary metabolite biosynthesis. This is characterized by modification of some transcriptional regulators for secondary metabolism development and the biosynthetic enzymes for secondary metabolite production.

Crotonylation positively regulates CCR of *Streptomyces*. *Streptomyces* is soil dwelling and has to compete with other microbes in the living community for nutrients, such as the chitin-degradative product *N*-acetyl-glucosamine⁵⁴. CCR has evolved in most microorganisms to use one carbon source in priority to support vegetative growth by suppressing the utilization of other carbon sources^{13,55}. For *Streptomyces*, glucose has been extensively used in laboratories as the main carbon source in

feast, and glucose-induced CCR has been shown to suppress bacterial differentiation, including morphogenesis and secondary metabolism development. Glk not only functions as a kinase to activate glucose in the first step of glucose catabolism but also has a regulatory role, proposed via a kind of PTM to interact with other transcriptional regulators, on CCR modulation^{13,20}.

Here we found that all enzymes are crotonylated in glucose catabolism, including glycolysis, pyruvate dehydrogenesis, and TCA, suggesting that crotonylation is involved in regulation of glucose utilization and subsequent CCR. Indeed, Over-crotonylation in a decrotonylase mutant $\Delta cobB$ not only increases Glk modification to reduce its kinase activity but also promotes total glucose consumption, suggesting that heavy crotonylation leads to high ratio of glucose uptake/Glk activity. Moreover, over-crotonylation suppresses the utilization of non-preferred carbon sources, indicating the intensified CCR. These observations suggested that high crotonylation will lead to CCR. We suspected that crotonylation might be one of the PTMs for Glk to interact with regulators to trigger CCR. So here we proposed that crotonylation modulates *Streptomyces* metabolism at least by positive regulation of CCR through dual regulation of Glk and carbon source metabolism. But the mechanism how crotonylation regulates interaction of Glk with other regulators still needs further investigation.

Crotonylation dynamics in regulation of *Streptomyces* metabolism. In this work, we showed that crotonylation during *Streptomyces* metabolism is properly controlled by a set of modification enzymes, including two decrotonylases CobB, HDAC, and one crotonyl-transferase Kct1. They play their roles in different development phases, as CobB mainly erases crotonylation during secondary metabolism, while HDAC and Kct1 work in the early stages. Abnormal crotonylation in these mutants results in altered patterns of cell growth and metabolite production, suggesting that the concerted crotonylation is essential for proper metabolism of *Streptomyces*.

Based on our understanding of crotonylation on regulation of CCR, we propose that gradually increasing modification of *Streptomyces* proteins can maintain CCR for continuous preferred carbon source (such as glucose as a model in the laboratory cultivation) utilization and vegetative growth. Since glucose drops rapidly in the medium in the early phases and loses its control on CCR, crotonylation can reinforce CCR to make sure that *Streptomyces* can keep consuming glucose in priority. This hypothesis is supported by the observation that the $\Delta kct1$ mutant has reduced cell growth accompanied by weakened CCR, as characterized by reduced glucose utilization and hyper-expression of genes for utilization of galactose. However, after vegetative growth, crotonylation needs to be partially erased to relieve CCR or reduce the modification of some regulators or biosynthetic enzymes for proper secondary metabolism development and efficient natural product biosynthesis, as block in hyper-crotonylation in the $\Delta cobB$ mutant is detrimental to secondary metabolite production.

In summary, here we showed that crotonylation, a previously unreported protein PTM, comprehensively regulates the metabolism of *Streptomyces*. Specifically, crotonylation positively regulates CCR for the proper development of *Streptomyces* metabolism. Our findings provide insights of PTM regulatory mechanisms on *Streptomyces* metabolism so far and the basis for possible molecular engineering of this modification system to take the full advantage of this genus for natural product development.

Methods

Strains, media, and biological materials. All strains used in this study are listed in Table 1. Wild-type *S. roseosporus* strain L30 was a daptomycin producer⁴⁰. All

the *S. roseosporus* mutants ($\Delta prcB/A$, $\Delta cobB$, $\Delta hdac$, $\Delta kct1$) were constructed based on the temperature-sensitive plasmid pKC1139⁴⁰. The plasmids were transferred into wild-type strain by conjugation⁴. After double cross-over, the genotypes were verified by PCR. *E. coli* DH5 α (Novagen) was the host for plasmid construction, and ET12567/pUZ8002 was used for conjugation to introduce DNA from *E. coli* to *S. roseosporus*⁴⁰. Proteins were expressed and purified from *E. coli* BL21 (DE3) (Novagen).

Liquid tryptic soy broth with 5% PEG6000 was the media for *S. roseosporus* mycelium preparation, and YEME (0.3% yeast extract, 0.3% malt extract, 0.5% tryptone, 4% glucose) was used for daptomycin production. R5 solid medium worked for sporulation, while MS solid medium was used for conjugation. All *E. coli* strains were cultured in LB medium⁴. Minimum medium (MM) (0.2% NH₄Cl, 0.1% (NH₄)₂SO₄, 0.05% KCl, 0.05% NaCl, 0.1% KH₂PO₄, 0.05% MgSO₄·7H₂O, 0.002% FeSO₄·7H₂O) was used for quantitative detection of transcription of related genes for other carbon utilization.

Plasmid construction. All plasmids and primers are provided in Table 2 and Supplementary Data 1, respectively. For construction of pKC1139-based plasmids for deletion, the left and right homologous fragments of *prcB/A*, *cobB*, *hdac*, *kct1*, and *glk* were amplified with primer pairs 1 + 2 and 3 + 4, 7 + 8 and 9 + 10, 13 + 14 and 15 + 16, 19 + 20 and 21 + 22, and 161 + 162 and 163 + 164 respectively, and sequentially recombined to pKC1139 digested with *XbaI/BamHI* by the ClonExpress MultiS One Step Cloning Kit (Vazyme, China). pET28a and pET32a vectors were used for protein expression in *E. coli*. The DNA fragment of *glk* was amplified with primer pair 25 + 26 and cloned into the *EcoRI/BamHI* site of pET32a to yield the plasmid pET32a-*glk*. The fragments of *cobB* (primers 33 + 34) and *kct1* (primers 35 + 36) were amplified and inserted into the *NdeI/BamHI* site of pET28a by the ClonExpress II One Step Cloning Kit (Vazyme). The expression vectors of Glk mutants were amplified from the plasmids pET32a-*glk* using primers 27–32 by PCR and confirmed by DNA sequencing. The fragment used for Bacterial Two-Hybrid System of *glk* (primers 39 + 40) was recombined to pUT18 digested with *XbaI/BamHI*. *cobB* (primers 41 + 42) and *kct1* (primers 43 + 44) were recombined to pKT25 digested with *XbaI/BamHI* by the ClonExpress II One Step Cloning Kit (Vazyme). *glk* was amplified with primer pair 37 + 38 and cloned into *XbaI/BglII* site of pSN7³⁷ by the ClonExpress II One Step Cloning Kit (Vazyme). All the fragments were amplified with KOD-Plus-Neo (Toyobo) using *S. roseosporus* L30 genomic DNA as the template.

Crotonyl-proteomic analysis of *Streptomyces* proteins. Identification of crotonylated proteins and the following in silico analysis were demonstrated by PTM Biolabs Inc. (Hangzhou, China). Detailed procedures are described in Supplementary Materials and Methods.

GO and KEGG analysis. GO annotation is a bioinformatics analysis method that can organically link various information of genes and gene products (such as proteins) to provide statistical information. GO annotations of proteome were derived from the UniProt-GOA database (<http://www.ebi.ac.uk/GOA/>). First, the system would convert the protein ID to UniProt ID, which would be used to match the GO ID. Next we retrieved the corresponding information from the UniProt-GOA database according to the GO ID. If there was no protein information in the UniProt-GOA database, an algorithm software based on protein sequences, InterProScan, would be used to predict the GO function of the protein. This protein was then classified according to cellular composition, molecular function, or physiological process. Then we used the KEGG pathway database to annotate protein pathways. First, we used the KEGG online service tool KAAS to annotate the submitted proteins and then used KEGG mapper to match the annotated proteins to the corresponding pathways in the database.

Construction of bacterial two-hybrid library. Fifty-four putative acyl-transferases and two de-acylases in two-hybrid library are listed in Supplementary Data 6. All fragments used for this library construction were recombined to *XbaI/BamHI*-digested pKT25 by ClonExpress II One Step Cloning Kit (Vazyme), and primers used are listed in Supplementary Data 1. Plasmids were transformed individually into *E. coli* BTH101, which was grown in LB media with kanamycin. A single colony from each plate was cultured in LB in 96-well clear flat bottom polystyrene microplates (Corning), mixed together, and saved in ultra-low temperature after overnight culture at 37 °C.

Metabolite analysis. The metabolites pyruvate and ATP were determined with the Pyruvate Assay Kit (Solarbio, BC2205) and ATP Assay Kit (Beyotime, S0026), respectively, according to the manufacturer's instructions. Daptomycin was analyzed as described previously⁴⁰.

Glk activity assays. Wild-type Glk and its mutant isoforms were expressed and purified from *E. coli* as previously described⁴⁰. Glk activity assays were performed at 30 °C for 10 min in Buffer A (20 mM Tris-HCl pH 8.0, 100 mM KCl, 7.5 mM MgCl₂, 2 mM DTT, 1 mM NAD⁺, 5 mM ATP, 0.1 M glucose, 0.4 U of glucose-6-phosphate dehydrogenase (Sangon Biotech, A003992)), and the signals were

Table 1 *Streptomyces* strains used in this study.

Strain	Description	Source or references
Wild type	<i>Streptomyces roseosporus</i> L30	40
$\Delta prcB/A$	In-frame deletion of <i>prcB/A</i> in wild type	This work
$\Delta cobB$	In-frame deletion of <i>cobB</i> in wild type	This work
$\Delta hdac$	In-frame deletion of <i>hdac</i> in wild type	This work
$\Delta kct1$	In-frame deletion of <i>kct1</i> in wild type	This work
Δglk	In-frame deletion of <i>glk</i> in wild type	This work
$\Delta glk::pSN7-glk$	Glk tagged with FLAG at N terminus, overexpressed under <i>ermEp*</i> in Δglk	This work
$\Delta glk::pSN7-glk(K8991Q)$	Glk(K8991Q) tagged with FLAG at N terminus, overexpressed under <i>ermEp*</i> in Δglk	This work
$\Delta glk::pSN7-glk(K8991R)$	Glk(K8991R) tagged with FLAG at N terminus, overexpressed under <i>ermEp*</i> in Δglk	This work
WT::pSN7- <i>glk</i>	Glk tagged with FLAG at N terminus and His at C terminus, overexpressed under <i>ermEp*</i> in wild type	This work
$\Delta cobB::pSN7-glk$	Glk tagged with FLAG at N terminus and His at C terminus, overexpressed under <i>ermEp*</i> in $\Delta cobB$	This work
$\Delta kct1::pSN7-glk$	Glk tagged with FLAG at N terminus and His at C terminus, overexpressed under <i>ermEp*</i> in $\Delta kct1$	This work
<i>S. coelicolor</i> M145	Wild type, SCP1 ⁻ , SCP2 ⁻	33
<i>S. lividans</i> TK24	Wild type	34
<i>S. albus</i> J1074	Wild type	35
<i>S. tsukubaensis</i> L19	Wild type	36

Table 2 Plasmids used in this study.

Plasmid	Description	References
pKC1139	Bifunctional <i>oriT</i> RK2 plasmid for gene deletion	40
pKC1139- $\Delta prcB/A$	<i>prcB/A</i> knockout plasmid based on pKC1139	This work
pKC1139- $\Delta cobB$	<i>cobB</i> knockout plasmid based on pKC1139	This work
pKC1139- $\Delta hdac$	<i>hdac</i> knockout plasmid based on pKC1139	This work
pKC1139- $\Delta kct1$	<i>kct1</i> knockout plasmid based on pKC1139	This work
pKC1139- Δglk	<i>glk</i> knockout plasmid based on pKC1139	This work
pET32a	Expression vector in <i>E. coli</i> with His tag	Novagen
pET32a- <i>glk</i>	<i>glk</i> in pET32a	This work
pET32a- <i>glk</i> (K89Q)	<i>glk</i> (K89Q) in pET32a	This work
pET32a- <i>glk</i> (K91Q)	<i>glk</i> (K91Q) in pET32a	This work
pET32a- <i>glk</i> (K8991Q)	<i>glk</i> (K8991Q) in pET32a	This work
pET28a	Expression vector in <i>E. coli</i> with His-tag	Novagen
pET28a- <i>cobB</i>	<i>cobB</i> in pET28a	This work
pET28a- <i>kct1</i>	<i>kct1</i> in pET28a	This work
pUT18	Vector for bacterial two-hybrid system	This work
pKT25	Vector for bacterial two-hybrid system	Euromedex
pUT18- <i>zip</i>	Control plasmid for bacterial two-hybrid system	Euromedex
pKT25- <i>zip</i>	Control plasmid for bacterial two-hybrid system	Euromedex
pUT18- <i>glk</i>	<i>glk</i> in pUT18	Euromedex
pKT25- <i>cobB</i>	<i>cobB</i> in pKT25	This work
pKT25- <i>kct1</i>	<i>kct1</i> in pKT25	This work
pSN7	Overexpression integrative shuttle vector containing <i>ermEp*</i> with 3×FLAG tag at N terminus and 18×His tag at C terminus	37
pSN7- <i>glk</i>	<i>glk</i> in pSN7	This work
pSN7- <i>glk</i> (K8991Q)	<i>glk</i> (K8991Q) in pSN7	This work
pSN7- <i>glk</i> (K8991R)	<i>glk</i> (K8991R) in pSN7	This work

determined by spectrophotometer at 340 nm. For analysis of Glk from *Streptomyces* lysate, 100 µg of cell extract was added to the reactions along with 1 mM phenylmethylsulfonyl fluoride (PMSF). For activity assays of Glk from *E. coli*, the reaction was carried out with 10 µg of Glk.

In vitro crotonylation and decrotonylation assays. Bacterial two hybrids for protein–protein interaction were performed with the Bacterial Adenylate Cyclase Two-Hybrid System Kit (Euromedex) according to the product manual. For in vitro crotonylation reaction, 1 µg of Kct1, 2 µg of Glk, and 10 mM of crotonyl-CoA (Sigma) were added in the reaction buffer (20 mM Tris-HCl (pH 8.0), 100 mM KCl, 7.5 mM MgCl₂) and incubated at 30 °C for 1.5 h, followed by Glk activity assays or loading for sodium dodecyl sulfate-polyacrylamide gel electrophoresis (SDS-PAGE). Decrotonylation assays were performed in the same reaction conditions, but 2.5 µg of Glk + 2 µg of CobB were used. The total loading protein and crotonylation were analyzed by western blot with antibodies against His-tag (Sigma) and crotonyllysine (Kcr) (PTM-502, PTM Biolabs Inc.) (1:2000), respectively.

In vivo decrotonylation assays by immunoprecipitation. The mycelia were collected and lysed in pre-cold phosphate-buffered saline (PBS) buffer by ultrasonication on ice. The remaining debris were removed by centrifugation at 12,000 rpm at 4 °C for 10 min. Twenty µl of anti-FLAG M2 affinity Gel (sigma, A2220) were added and incubated for 3 h in a roller shaker. The resin was centrifuged for 2 min at 5000 ×g, and the supernatant was removed. After wash with PBS buffer for three times, the immunoprecipitated complexes were boiled in 1× loading buffer (62.5 mM Tris-HCl (pH 6.8), 2% SDS, 10% (v/v) glycerol, and 0.002% bromophenol blue), subjected to SDS-PAGE, and immunoblotted with anti-Kcr (PTM-501, PTM Biolabs Inc.) or anti-FLAG (M2, Sigma) antibody (1:2000).

RNA preparation and quantitative real-time PCR (qRT-PCR). RNA was prepared from mycelia with the RN43-EASYspin Plus Kit (Aidlab Biotech Co., Ltd. China) according to the manufacturer's protocol. Genomic DNA was removed with RNase-free DNase I (TaKaRa), and cDNA was prepared with MMLV (TaKaRa) as described by the supplier. qRT-PCR was performed with SYBR Premix Ex Taq II (TaKaRa) for genes *hrdB*, *dptE*, and *galK* with primer pairs 45 + 46,

47 + 48, and 49 + 50, respectively. The relative fold changes of gene expression were calculated based on the formula of $2^{-\Delta\Delta C_t}$.

LC-MS analysis of crotonyl-CoA and acetyl-CoA. Mycelia were collected and lysed in PBS supplemented with 1 mM PMSF. The remaining debris was removed by centrifugation at 10,000 rpm at 4 °C for 5 min, and the protein was precipitated with cold 20% TCA for 2 h at -20 °C. After centrifugation at 10,000 rpm at 4 °C for 10 min, the supernatant was transferred to a new centrifuge tube. Crotonyl-CoA and acetyl-CoA was further purified with an Oasis PRiME HLB 96-well Plate and 30 mg of Sorbent per Well (Waters, 186008054) according to the manufacturer's instructions. Finally, effluent was concentrated on the CentriVap vacuum (Lab-conco) and subjected to LC-MS on an Agilent Eclipse TC-C18 column (5 µm, 4.6×250 mm, Agilent Technologies), at a flow rate of 0.5 ml/min. Solution A (water containing 20 mM ammonium acetate, pH = 7.4) and solution B (methanol with 20 mM ammonium acetate) were employed to isolate the components with ultraviolet detection set at 254 nm. Elution was initiated with constant 25% solvent B for 5 min and then performed with a linear gradient from 25% to 100% of solvent B in 20 min, followed by 100% solvent B for 5 min and re-equilibration to initial conditions for 5 min. The MS system was operated with an electrospray ionization source in positive ion mode³².

Statistics and reproducibility. All statistics underlying the graphs and charts were analyzed by Excel 2017 and Prism (version 5, GraphPad). All experiments were independently performed in triplicate at least, indicated in the corresponding figure legend. Images were combined and annotated in Adobe Photoshop (version 2019).

Reporting summary. Further information on research design is available in the Nature Research Reporting Summary linked to this article.

Data availability

All data supporting the findings of the current study are available within the article and Supplementary Information or from the corresponding authors upon request. Full blots and the mass spectrometric data for the modification peptides and residues are provided in Supplementary Information. The source data underlying plots shown in figures are shown in Supplementary Data 7.

Received: 28 August 2019; Accepted: 31 March 2020;

Published online: 24 April 2020

References

- Berdy, J. Bioactive microbial metabolites. *J. Antibiot. (Tokyo)* **58**, 1–26 (2005).
- Barajas, J. F., Blake-Hedges, J. M., Bailey, C. B., Curran, S. & Keasling, J. D. Engineered polyketides: synergy between protein and host level engineering. *Synth. Syst. Biotechnol.* **2**, 147–166 (2017).
- Xu, J. Y. et al. Protein acylation is a general regulatory mechanism in biosynthetic pathway of acyl-CoA-derived natural products. *Cell Chem. Biol.* **25**, 984–995 (2018).
- Angell, S., Lewis, C. G., Buttner, M. J. & Bibb, M. J. Glucose repression in *Streptomyces coelicolor* A3(2): a likely regulatory role for glucose kinase. *Mol. Gen. Genet.* **244**, 135–143 (1994).
- van Wezel, G. P. & McDowall, K. J. The regulation of the secondary metabolism of *Streptomyces*: new links and experimental advances. *Nat. Prod. Rep.* **28**, 1311–1333 (2011).
- Niu, G., Chater, K. F., Tian, Y., Zhang, J. & Tan, H. Specialised metabolites regulating antibiotic biosynthesis in *Streptomyces* spp. *FEMS Microbiol. Rev.* **40**, 554–573 (2016).
- Liu, G., Chater, K. F., Chandra, G., Niu, G. Q. & Tan, H. R. Molecular regulation of antibiotic biosynthesis in *Streptomyces*. *Microbiol. Mol. Biol. Rev.* **77**, 112–143 (2013).
- Mikulik, K. et al. CobB1 deacetylase activity in *Streptomyces coelicolor*. *Biochem. Cell Biol.* **90**, 179–187 (2012).
- Tucker, A. C. & Escalante-Semerena, J. C. Acetoacetyl-CoA synthetase activity is controlled by a protein acetyltransferase with unique domain organization in *Streptomyces lividans*. *Mol. Microbiol.* **87**, 152–167 (2013).
- Liao, G., Xie, L., Li, X., Cheng, Z. & Xie, J. Unexpected extensive lysine acetylation in the trump-card antibiotic producer *Streptomyces roseosporus* revealed by proteome-wide profiling. *J. Proteomics* **106**, 260–269 (2014).
- Ishigaki, Y. et al. Protein acetylation involved in streptomycin biosynthesis in *Streptomyces griseus*. *J. Proteomics* **155**, 63–72 (2017).
- Swiatek, M. A. et al. The ROK family regulator Rok7B7 pleiotropically affects xylose utilization, carbon catabolite repression, and antibiotic production in *Streptomyces coelicolor*. *J. Bacteriol.* **195**, 1236–1248 (2013).
- Romero-Rodriguez, A. et al. Carbon catabolite regulation in *Streptomyces*: new insights and lessons learned. *World J. Microbiol. Biotechnol.* **33**, 162 (2017).
- Sanchez, S. et al. Carbon source regulation of antibiotic production. *J. Antibiot. (Tokyo)* **63**, 442–459 (2010).
- Ordóñez-Robles, M. et al. *Streptomyces tsukubaensis* as a new model for carbon repression: transcriptomic response to tacrolimus repressing carbon sources. *Appl. Microbiol. Biotechnol.* **101**, 8181–8195 (2017).
- Gubbens, J., Janus, M. M., Florea, B. I., Overkleeft, H. S. & van Wezel, G. P. Identification of glucose kinase-dependent and -independent pathways for carbon control of primary metabolism, development and antibiotic production in *Streptomyces coelicolor* by quantitative proteomics. *Mol. Microbiol.* **86**, 1490–1507 (2012).
- Romero-Rodriguez, A. et al. Transcriptomic analysis of a classical model of carbon catabolite regulation in *Streptomyces coelicolor*. *BMC Microbiol.* **16**, 77 (2016).
- Ramos, I. et al. Glucose kinase alone cannot be responsible for carbon source regulation in *Streptomyces peucetius* var. *caesius*. *Res. Microbiol.* **155**, 267–274 (2004).
- Kwakman, J. H. J. M. & Postma, P. W. Glucose kinase has a regulatory role in carbon catabolite repression in *Streptomyces coelicolor*. *J. Bacteriol.* **176**, 2694–2698 (1994).
- van Wezel, G. P. et al. A new piece of an old jigsaw: glucose kinase is activated posttranslationally in a glucose transport-dependent manner in *Streptomyces coelicolor* A3(2). *J. Mol. Microbiol. Biotechnol.* **12**, 67–74 (2007).
- Tan, M. et al. Identification of 67 histone marks and histone lysine crotonylation as a new type of histone modification. *Cell* **146**, 1016–1028 (2011).
- Suzuki, Y., Horikoshi, N., Kato, D. & Kurumizaka, H. Crystal structure of the nucleosome containing histone H3 with crotonylated lysine 122. *Biochem. Biophys. Res. Commun.* **469**, 483–489 (2016).
- Wei, W. et al. Class I histone deacetylases are major histone decrotonylases: evidence for critical and broad function of histone crotonylation in transcription. *Cell Res.* **27**, 898–915 (2017).
- Ruiz-Andres, O. et al. Histone lysine crotonylation during acute kidney injury in mice. *Dis. Model. Mech.* **9**, 633–645 (2016).
- Xu, W. et al. Global profiling of crotonylation on non-histone proteins. *Cell Res.* **27**, 946–949 (2017).
- Liu, K. et al. A qualitative proteome-wide lysine crotonylation profiling of papaya (*Carica papaya* L.). *Sci. Rep.* **8**, 8230 (2018).
- Kwon, O. K., Kim, S. J. & Lee, S. First profiling of lysine crotonylation of myofibrillar proteins and ribosomal proteins in zebrafish embryos. *Sci. Rep.* **8**, 3652 (2018).
- Sun, H. et al. First comprehensive proteome analysis of lysine crotonylation in seedling leaves of *Nicotiana tabacum*. *Sci. Rep.* **7**, 3013 (2017).
- Narita, T., Weinert, B. T. & Choudhary, C. Functions and mechanisms of non-histone protein acetylation. *Nat. Rev. Mol. Cell Biol.* **20**, 156–174 (2019).
- Sabari, B. R., Zhang, D., Allis, C. D. & Zhao, Y. Metabolic regulation of gene expression through histone acylations. *Nat. Rev. Mol. Cell Biol.* **18**, 90–101 (2017).
- Seto, E. & Yoshida, M. Erasers of histone acetylation: the histone deacetylase enzymes. *Cold Spring Harb. Perspect. Biol.* **6**, a018713 (2014).
- Sabari, B. R. et al. Intracellular crotonyl-CoA stimulates transcription through p300-catalyzed histone crotonylation. *Mol. Cell* **58**, 203–215 (2015).
- Mao, X. M. et al. Proteasome involvement in a complex cascade mediating SigT degradation during differentiation of *Streptomyces coelicolor*. *FEBS Lett.* **588**, 608–613 (2014).
- Ruckert, C. et al. Complete genome sequence of *Streptomyces lividans* TK24. *J. Biotechnol.* **199**, 21–22 (2015).
- Zaburannyi, N., Rabyk, M., Ostash, B., Fedorenko, V. & Luzhetskyy, A. Insights into naturally minimised *Streptomyces albus* J1074 genome. *BMC Genomics* **15**, 97 (2014).
- Zhang, X. S. et al. FkbN and Tcs7 are pathway-specific regulators of the FK506 biosynthetic gene cluster in *Streptomyces tsukubaensis* L19. *J. Ind. Microbiol. Biotechnol.* **43**, 1693–1703 (2016).
- Erb, T. J. et al. Synthesis of C5-dicarboxylic acids from C2-units involving crotonyl-CoA carboxylase/reductase: the ethylmalonyl-CoA pathway. *Proc. Natl Acad. Sci. USA* **104**, 10631–10636 (2007).
- Striebel, F., Imkamp, F., Ozelik, D. & Weber-Ban, E. Pupylation as a signal for proteasomal degradation in bacteria. *Biochim. Biophys. Acta* **1843**, 103–113 (2014).
- Ohnishi, Y., Yamazaki, H., Kato, J. Y., Tomono, A. & Horinouchi, S. AdpA, a central transcriptional regulator in the A-factor regulatory cascade that leads to morphological development and secondary metabolism in *Streptomyces griseus*. *Biosci. Biotechnol. Biochem.* **69**, 431–439 (2005).
- Mao, X. M. et al. Transcriptional regulation of the daptomycin gene cluster in *Streptomyces roseosporus* by an autoregulator, AtrA. *J. Biol. Chem.* **290**, 7992–8001 (2015).

41. Hesketh, A., Chen, W. J., Ryding, J., Chang, S. & Bibb, M. The global role of ppGpp synthesis in morphological differentiation and antibiotic production in *Streptomyces coelicolor* A3(2). *Genome Biol.* **8**, R161 (2007).
42. He, J. M. et al. Direct involvement of the master nitrogen metabolism regulator GlnR in antibiotic biosynthesis in *Streptomyces*. *J. Biol. Chem.* **291**, 26443–26454 (2016).
43. Zheng, Y. et al. Dual regulation between the two-component system PhoRP and AdpA regulates antibiotic production in *Streptomyces*. *J. Ind. Microbiol. Biotechnol.* **46**, 725–737 (2019).
44. Miao, V. et al. Daptomycin biosynthesis in *Streptomyces roseosporus*: cloning and analysis of the gene cluster and revision of peptide stereochemistry. *Microbiology* **151**, 1507–1523 (2005).
45. Huang, D., Li, Z. H., You, D., Zhou, Y. & Ye, B. C. Lysine acetylproteome analysis suggests its roles in primary and secondary metabolism in *Saccharopolyspora erythraea*. *Appl. Microbiol. Biotechnol.* **99**, 1399–1413 (2015).
46. Colak, G. et al. Identification of lysine succinylation substrates and the succinylation regulatory enzyme CobB in *Escherichia coli*. *Mol. Cell. Proteomics* **12**, 3509 (2013).
47. Kelly, R. D. W. et al. Histone deacetylase (HDAC) 1 and 2 complexes regulate both histone acetylation and crotonylation *in vivo*. *Sci. Rep.* **8**, 14690 (2018).
48. Zhao, S., Zhang, X. & Li, H. Beyond histone acetylation-writing and erasing histone acylations. *Curr. Opin. Struct. Biol.* **53**, 169–177 (2018).
49. Lu, Y. X., Liu, X. X., Liu, W. B. & Ye, B. C. Identification and characterization of two types of amino acid-regulated acetyltransferases in actinobacteria. *Biosci. Rep.* **37**, BSR20170157 (2017).
50. Dong, H. Y., Zhai, G. J., Chen, C., Bai, X., Tian, S. S., Hu, D. Q., Fan, E. G. & Zhang, K. Protein lysine de-2-hydroxyisobutyrylation by CobB in prokaryotes. *Sci. Adv.* **5**, 13 (2019).
51. Miyazono, K. et al. Substrate recognition mechanism and substrate-dependent conformational changes of an ROK family glucokinase from *Streptomyces griseus*. *J. Bacteriol.* **194**, 607–616 (2012).
52. Urem, M., Swiatek-Polatynska, M. A., Rigali, S. & van Wezel, G. P. Intertwining nutrient-sensory networks and the control of antibiotic production in *Streptomyces*. *Mol. Microbiol.* **102**, 183–195 (2016).
53. Adams, C. W., Fornwald, J. A., Schmidt, F. J., Rosenberg, M. & Brawner, M. E. Gene organization and structure of the *Streptomyces lividans gal* operon. *J. Bacteriol.* **170**, 203–212 (1988).
54. Świątek, M. A., Urem, M., Tenconi, E., Rigali, S. & van Wezel, G. P. Engineering of *N*-acetylglucosamine metabolism for improved antibiotic production in *Streptomyces coelicolor* A3(2) and an unsuspected role of NagA in glucosamine metabolism. *Bioengineered* **3**, 6 (2012).
55. Gorke, B. & Stulke, J. Carbon catabolite repression in bacteria: many ways to make the most out of nutrients. *Nat. Rev. Microbiol.* **6**, 613–624 (2008).

Acknowledgements

We gratefully thank Professor Yu-Feng Yao in Shanghai Jiaotong University for his critical help in bacterial two-hybrid system and useful discussion on PTMs. This work was financially supported by National Natural Science Foundation of China (NSFC) (3173002, 31520103901) to Y.-Q.L. and the National Key R&D Program (2019YFA0905400) and NSFC (31571284) to X.-M.M.

Author contributions

X.-M.M., Y.-Q.L., and X.-A.C. conceived the project. X.-M.M. and C.-F.S. designed the experiments. C.-F.S., Q.-W.Z., and W.-F.X. performed the experiments. All the authors analyzed the data. C.-F.S., Y.-Q.L., and X.-M.M. wrote and edited the manuscript.

Competing interests

The authors declare no competing interests.

Additional information

Supplementary information is available for this paper at <https://doi.org/10.1038/s42003-020-0924-2>.

Correspondence and requests for materials should be addressed to Y.-Q.L. or X.-M.M.

Reprints and permission information is available at <http://www.nature.com/reprints>

Publisher's note Springer Nature remains neutral with regard to jurisdictional claims in published maps and institutional affiliations.



Open Access This article is licensed under a Creative Commons Attribution 4.0 International License, which permits use, sharing, adaptation, distribution and reproduction in any medium or format, as long as you give appropriate credit to the original author(s) and the source, provide a link to the Creative Commons license, and indicate if changes were made. The images or other third party material in this article are included in the article's Creative Commons license, unless indicated otherwise in a credit line to the material. If material is not included in the article's Creative Commons license and your intended use is not permitted by statutory regulation or exceeds the permitted use, you will need to obtain permission directly from the copyright holder. To view a copy of this license, visit <http://creativecommons.org/licenses/by/4.0/>.

© The Author(s) 2020